

Novel hydrogels containing Nafion and poly(ethylene oxide) based block copolymers

D. Fernandes^a, W. Kluska^a, J. Stanislawska^a, B. Board^a, M. J. Krysmann^b and A. Kelarakis^{a*}

^a Centre for Materials Science, School of Physical Sciences and Computing, University of Central Lancashire, Preston PR12HE, U.K.

^b School of Pharmacy and Biosciences, University of Central Lancashire, Preston PR12HE, U.K.

email: akelarakis@uclan.ac.uk, tel: 004417724172

Abstract

We present a novel family of biocompatible hydrogels containing Nafion and poly(ethylene oxide) based block copolymers. In aqueous environment, thermodynamically stable ionomer-copolymer complexes are formed, as evident by light scattering and quartz crystal microbalance experiments. Moreover, incorporation of Nafion dramatically modifies the phase behaviour and the rheological properties of copolymer hydrogels. The hybrid systems not only undergo sharp and thermally reversible sol-gel transitions below the body temperature, thus retaining their injectable nature, but they also generate mechanically robust hydrogels. Moreover, ibuprofen was continuously released over a period of 26 days for the Nafion/Pluronic hydrogel, compared to only 3 days for the Nafion-free system. The hybrid gels are promising candidates for 3D-bioprinting and controlled drug release applications.

keywords: Nafion; Pluronics; poly(ethylene oxide); hydrogels; injectable; drug release.

Introduction

Hydrogels are water swollen networks of chemically or physically crosslinked macromolecular chains having a highly porous structure that exhibit complex viscoelastic characteristics¹⁻³. The physical properties of those soft systems can be largely tuned with respect to the chemical composition of the polymeric components and their crosslinking density. Stimuli-

responsive hydrogels can sense and adapt to changes in their surroundings such as temperature, pH, ionic strength, pressure, light, electric field and the presence of certain chemical triggers^{4,5}.

Particular emphasis is given to the development of injectable systems^{6,7} that gel *in situ* under physiological conditions facilitating the controlled and sustained release of the entrapped drugs. Because they

can be applied in nonsurgical treatments (tissue engineering, drug delivery, wound repair, dermal filling, etc.), they offer obvious advantages in terms of therapy cost and duration as well as patient comfort and recovery. Injectable hydrogels are derived by natural polymers (such as hyaluronic acid⁸, cellulose⁹, proteins and peptides¹⁰, chitosan¹¹) or synthetic macromolecules (composed of acrylates methacrylates, vinyl ethers, cyclic esters, amino acids, acrylamides, etc.)¹².

The dynamic presence of poly(ethylene oxide) (PEO) based copolymers in the field of injectable hydrogels can be traced back to their interesting self-assembly properties that allow sharp sol-gel thermoreversible transitions below body temperature^{13,14}. This class of nanostructured gels exhibit minimal cytotoxicity and improved pharmacokinetics¹⁵, but they typically suffer from weak mechanical properties and rapid drug release. Well-explored approaches to overcome those challenges rely on the development of photocrosslinked¹⁶, stereocomplexed¹⁷ and multicomponent¹⁸ systems.

In this report we demonstrate that introduction of Nafion to hydrogels containing PEO based copolymers improves their drug release profile and enhances their mechanical strength, without compromising their injectable character. Nafion is primarily known as the proton exchange membrane in fuel cells^{19,20}. Early studies have demonstrated its biocompatible nature^{21,22}, but it has only recently attracted significant attention for biomedical applications such as implant coatings²³, biosensors^{24,25} and biocompatible capsules²⁶. Its amphiphilic structure consists of a remarkably robust Teflon-like backbone

decorated with highly polar pendant groups. Due to this macromolecular design, Nafion interacts strongly with non-ionic block copolymers^{27,28} giving rise to thermodynamically stable supramolecular assemblies.

2. Experimental Section

2.1. Materials

Two Nafion dispersions (in water and low aliphatic alcohols, respectively) were obtained by Ion Power. Pluronic P123 was obtained by Sigma Aldrich and is referred here as E₁₉P₆₉E₁₉. The notations are as follows: E stands for an oxyethylene unit OCH₂CH₂, P for oxypropylene OCH₂CH(CH₃), while the subscripts denote number-average block of repeat units. The copolymer B₂₀E₅₁₀, where B stands for an oxybutylene unit OCH₂CH(C₂H₅), was synthesized by sequential anionic polymerization of 1,2-butylene oxide followed by ethylene oxide, using potassium activated 2-butanol as initiator²⁹.

2.2. Methods

2.2.1. Dynamic Light Scattering (DLS). DLS measurements at T= 25 °C were conducted using a Malvern Zetasizer Nano-ZS (Malvern Instruments, England) system equipped with a He-Ne laser beam with $\lambda = 633$ nm. Prior to the measurements the samples were filtered through Nylon membrane filters with a pore size of 0.2 μm directly to the measuring cuvettes.

2.2.2. Quartz Crystal Microbalance with dissipation monitoring (QCM-D). QCM-D experiments were conducted at T= 25 °C using a Q-sense E1 unit. SiO₂ modified crystals with fundamental resonance frequency close to 5 MHz were coated with

Nafion. To that end, a drop of ethanol containing 0.5 wt% Nafion was deposited in each crystal that was subsequently left for at least 48 h at room temperature to ensure complete evaporation of the solvent. The thus prepared Nafion-coated crystals were mounted to a flow cell (flow rate= 0.2 ml/min) and their interaction with water and copolymer solutions were monitored. When a layer of material with mass Δm is deposited on the crystal surface, its resonant frequency is reduced by Δf according to Sauerbrey relation³⁰

$$\Delta m = - (C/N) \Delta f \quad (1)$$

where N denotes the overtone number and C the integrated crystal sensitivity. The dissipation factor D is defined as

$$D = E_d / (2\pi E_s) \quad (2)$$

where E_d is the energy dissipated during one period of oscillation and E_s is the energy stored in the system³¹. For simplicity, only the third overtones (N=3) are described in this report.

2.2.3. Rheology. The viscoelastic properties of the hydrogels were studied using a stress controlled AR-G2 rheometer (TA). All measurements were performed within the linear viscoelastic region (strain 2%), using a parallel plate cell with 50 mm diameter. Frequency sweep data were collected at selected temperatures, while temperature ramps were performed at $\omega=1$ rad/sec with a heating rate of 1 °C/min. Extra care was taken to minimize evaporation by using a solvent trap to maintain a water saturated environment.

2.2.4. Small Angle X-ray Scattering (SAXS). SAXS experiments were performed on beamline I22, Diamond Light Source Synchrotron Radiation Source, U.K. The

wavelength of synchrotron radiation was 1 Å and the sample-to-detector distance was 6 m. Samples were mounted between mica windows in a liquid cell equipped with water-bath temperature control. Two dimensional SAXS patterns were collected using a Pilatus P3-2M area detector. All patterns were corrected for the incident beam fluctuations as well as air and instrument scattering, before being converted into 1D profiles using the Dawn software.

2.2.5. Drug release profiles. A gel containing 32.5 wt% E₁₉P₆₉E₁₉ and 0.5 wt% ibuprofen (Sigma- Aldrich) was transferred into a Snakeskin dialysis membrane (with molecular weight cut-off 3.5 kDa) and was subsequently immersed in phosphate buffer saline solution (pH 7.4) at a constant temperature of 37 °C. Samples of the buffer solution were withdrawn at predetermined times and the ibuprofen content was determined on a basis of a calibration curve using a Shimadzu UV3600 UV-Vis, at 265 nm. An, otherwise identical, experiment was conducted for the gel containing 32.5 wt% E₁₉P₆₉E₁₉ and 10 wt% Nafion.

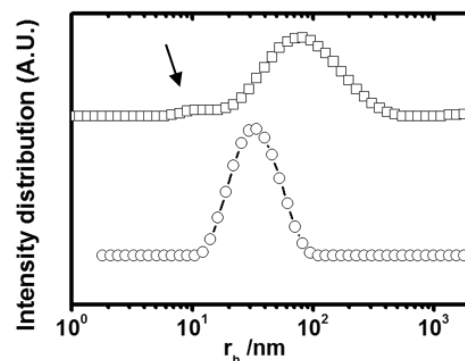


Figure 1 - Intensity fraction distributions of apparent hydrodynamic radius (r_h) at T= 25 °C for aqueous solutions of 0.5 wt % B₂₀E₅₁₀ in the absence (circles) and in the presence (squares) of 0.5 wt % Nafion. For clarity, the curves are displayed in the ordinate.

Results and discussion

Intensity fraction distributions of apparent hydrodynamic radius (r_h) of 0.5 wt % B₂₀E₅₁₀ aqueous solutions (circles in Figure 1) indicate the presence of highly swollen micelles with $r_h=31$ nm, in agreement with previous studies²⁹. Judging by its B block length¹⁴, the critical micelle concentration (cmc) of B₂₀E₅₁₀ is expected to fall below 10⁻⁴ wt%, consistent with the absence of a unimer peak. Addition of 0.5 wt% Nafion results in particles with $r_h=80$ nm (squares in Figure 1), an effect that suggests extensive Nafion-copolymer binding. For reference, a 0.5 wt % aqueous dispersion of Nafion shows a wide size distribution below 20 nm (data not shown here) and unbound Nafion particles might count for the minor peak observed in Figure 1.

Previous reports^{27,28} provide clear evidence that Nafion forms supramolecular assemblies with E₁₈B₁₀, E₁₉P₆₉E₁₉ and M₁₈E₂₀ (M₁₈ stands for C₁₈H₃₇) in water. For example, the critical micelle temperature (cmt) of E₁₉P₆₉E₁₉ solutions was found to systematically increase in the presence of Nafion, indicating strong copolymer adsorption to the ionomer backbone²⁷. The complexation has been attributed to hydrophobic interactions and extensive hydrogen bonding between Nafion's protons and the ether oxygen of EO³². It is interesting to note the architectural similarity between the copolymer's hydrophilic building block - OCH₂CH₂- and Nafion's side chain - OCF₂CF₂-.

Each one of the QCM-D sensorgrams in Figure 2 describes an initial equilibrium of a Nafion coated crystal against air in order to determine the fundamental resonance frequency, followed by a subsequent equilibrium against flowing water to

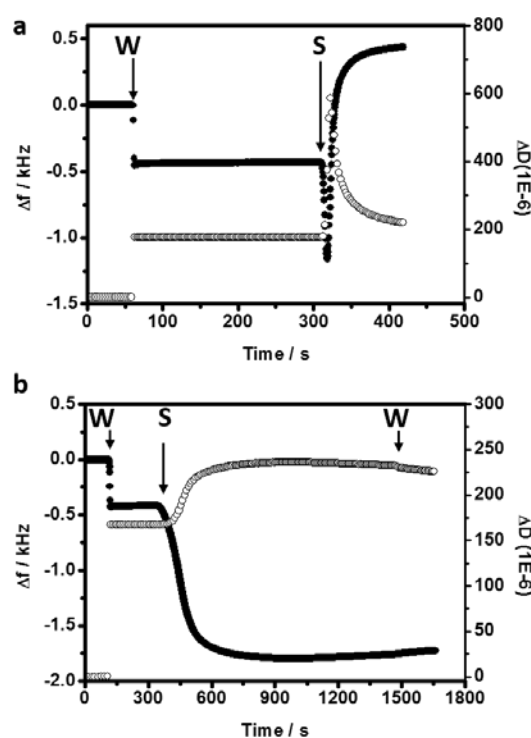


Figure 1 - Time course of frequency (filled symbols) and dissipation factor (open symbols) of a Nafion-coated crystal resonator in QCM-D experiments at 25 °C. "W" and "S" denote the injection of water and the copolymer solutions containing 0.5 wt% E₁₉P₆₉E₁₉ (a) and 0.5 wt% B₂₀E₅₁₀ (b), respectively.

determine the baseline of the hydrated membrane. The pronounced drop in f that follows the hydration of the crystals reveals the ample water uptake of the Nafion's ionic domains that does not, however, result in the dissolution of the membrane.

Introduction of 0.5 wt% E₁₉P₆₉E₁₉ solution (Figure 2a) to the hydrated Nafion membrane initially causes a dramatic decrease in f due to extensive copolymer adsorption, an effect that reduces the rigidity of the membrane as revealed by the accompanying increase in D . When the amount of the attached polymer exceeds a critical threshold, a rapid increase in f is observed due to the dissolution of the Nafion membrane. The detergency efficiency of E₁₉P₆₉E₁₉ against Nafion ultrathin membranes has been described in detail

previously^{27,28}, and the underlying mechanism holds true for E₁₈B₁₀ and M₁₈E₂₀.

Introduction of B₂₀E₅₁₀ solution (Figure 2b) also gives rise to a significant decrease in f and an accompanying increase in D , indicating rapid and extensive Nafion-copolymer binding. By virtue of their super-swollen nature ($r_h=31$ nm), the adsorbed copolymer chains impose significant steric constraints so that the rather limited amount of copolymer attached is incapable in solubilising Nafion. It has been estimated that each E-unit in the corona of B₂₀E₅₁₀ micelles is associated with 96 water molecules³³, out of which only 6 water molecules are present in the hydration layer³⁴ and the remaining is essentially bulk water. Nevertheless, QCM-D sensorgram suggest that B₂₀E₅₁₀ chains are firmly adsorbed to Nafion's surface and are not detached upon prolonged water rinsing. In contrast, in an otherwise identical experiment, it was found that a significant portion of the attached PEO on the Nafion membrane can be removed under water flow²⁷. The difference between the two systems, highlight the role of hydrophobic-hydrophobic interactions between the substrate and the adsorbed B₂₀E₅₁₀ chains that are not present in the case of PEO (that lacks hydrophobic groups).

The sol-gel phase diagram of concentrated aqueous dispersions of PEO based block copolymers is governed by the exothermic dissolution of ethylene glycol that favours micellization and, thereby, micellar packing at intermediate temperatures, but also accounts for pronounced corona dehydration and collapse of the close packing at elevated temperatures. As shown in Figure 3, upon heating the 32.5 wt% E₁₉P₆₉E₁₉ aqueous dispersion exhibits a sharp sol- gel transition at 19 °C (G' exceeds 1 kPa and $G'>G''$) and the structure collapses at 42 °C into a soft gel phase (G' falls much below 1 kPa, but

remains higher than G''). Soft gels are described as defected closely packed systems, where interacting micellar aggregates give rise to a moderate viscoelastic response (e.g. stronger than sol, but weaker than a hard gel)³⁵.

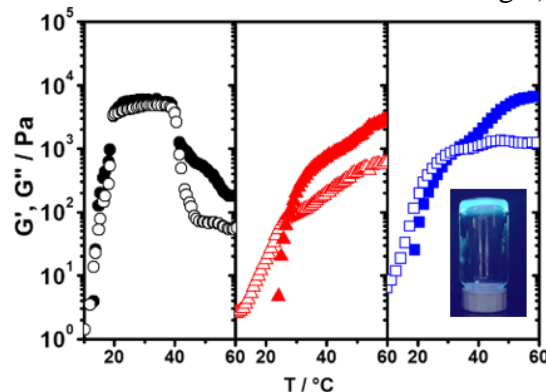


Figure 3 - Temperature sweeps ($\omega= 1$ rad/s, strain amplitude=2%) for aqueous gels containing 32.5 wt% E₁₉P₆₉E₁₉ in the absence (black circles) and the presence of 5wt% Nafion (red triangles) and 10 wt% Nafion (blue squares). Solid symbols denote storage modulus (G') and open symbols denote loss modulus (G''). The inset shows a photo of the gel containing 32.5 wt% E₁₉P₆₉E₁₉/10 wt% Nafion at 40 °C (a fluorescence dye has been added to facilitate imaging under UV radiation).

Addition of 5 wt% and 10 wt% Nafion modifies the phase diagram, given that the hybrid systems remain within the sol phase at temperatures up to 45 and 34 °C (G' exceeds 1 kPa and $G'>G''$), respectively and the gels formed are stable up to the highest temperature tested (60 °C). The inset shown in Figure 3 demonstrates a tube inversion test and shows the immobile nature of a 32.5 wt% E₁₉P₆₉E₁₉/10wt% Nafion gel at 40 °C. Significantly, the sol-gel transitions observed for the hybrid systems are thermoreversible and they remain unaltered upon repetitive heat-cool-heat cycles. In other words, while Pluronic hydrogels tend to exhibit a sol-gel-sol transition upon heating, addition of Nafion leads to a monotonous enhancement of viscoelasticity as a function of temperature. For reference, we note that a 13.9 wt% aqueous dispersion of the thermo and pH responsive linear triblock copolymer, poly(methoxydi(ethylene glycol) methacrylate-co-methacrylic acid)-b-PEO-b poly(methoxydi(ethylene glycol) methacrylate-co-methacrylic acid) at pH=4 undergoes sol-gel transition at 36.1 °C and

maintains a plateau G' value close to 3 kPa at least up to 65 °C³⁶.

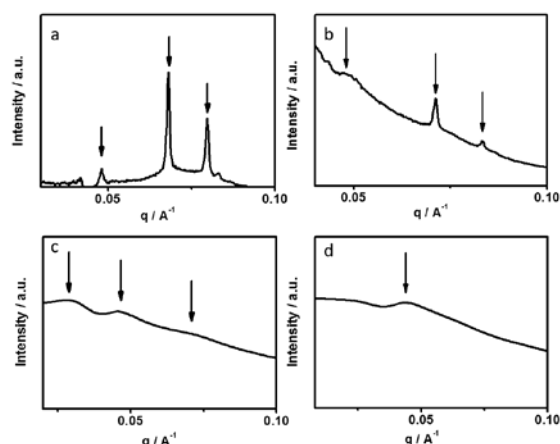


Figure 4 - SAXS patterns of aqueous gels of 32.5 wt% $E_{19}P_{69}E_{19}$ in the absence of Nafion (a) and in the presence of 1 wt% Nafion (b), 5 wt% Nafion (c) and 10 wt% Nafion (d).

The SAXS patterns shown in Figure 4 indicate a body centered cubic (bcc) packing for 32.5 wt% $E_{19}P_{69}E_{19}$ at 20 °C with reflections at $q/q^*=1:\sqrt{2}:\sqrt{3}$, where q stands for the scattering vector and q^* for the first order reflection³⁷. The bcc structure is somewhat maintained in the presence of 1wt% Nafion, although the hybrid is a weaker gel. Addition of 5 wt% Nafion has a profound impact, leading to a fluid system with broad scattering peaks ($q/q^*=1:\sqrt{3}:\sqrt{7}$) that are roughly consistent with hexagonal packing of cylinders³⁸. Moreover, in the presence of 10 wt% Nafion the fluid system does not possess any long range correlation. The dramatic effects induced by Nafion to the phase behaviour of the gels are in line with the extensive adsorption of $E_{19}P_{69}E_{19}$ to Nafion backbone, an effect that reduces the effective volume fraction of the dispersed particles, ultimately removing the close packing constrains. We note that SAXS profiles at 45 °C and 65 °C indicated the absence of an ordered structure for all hydrogels in the absence and in the presence of 5 and 10 wt% Nafion.

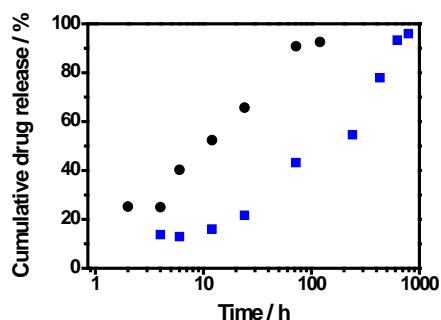


Figure 5 - Release profiles of ibuprofen from 32.5wt% $E_{19}P_{69}E_{19}$ in the absence (black circles) and presence (blue squares) of 10 wt% Nafion against phosphate buffer solution (pH=7.4) at 37 °C.

Figure 5 shows the release profiles of ibuprofen from 32.5 wt% $E_{19}P_{69}E_{19}$ in the absence (black circles) and presence (blue squares) of 10 wt% Nafion against phosphate buffer (pH=7.4) solution at 37 °C. A rather rapid release is observed from the copolymer gel given that 65 and 91 wt% of the drug was released within the first 24 and 72 h, respectively. For reference we note, that aceclofenac and paclitaxel are fully released within 24 h from a Pluronic micellar solution³⁹ and a Pluronic hydrogel⁴⁰, respectively. However, the diffusion of ibuprofen from the hybrid hydrogel is much slower given that 21, 55 and 93 wt% of the drug is released after 24, 240 and 624 h, respectively. Taking into account that the two systems have similar rheological properties at 37 °C (Figure 3), the improved release profile seen for the hybrid system can be attributed to a lower level of porosity/higher tortuosity or stronger matrix-drug interactions in the presence of Nafion. Further work is underway to elucidate the diffusion mechanism in this complex system. In a control experiment we investigated the drug release profile from an acidified 32.5 wt% Pluronic gel (pH=3, in accordance to that measured for the Nafion/Pluronic gel), but the effect of pH adjustment was found to be minimal.

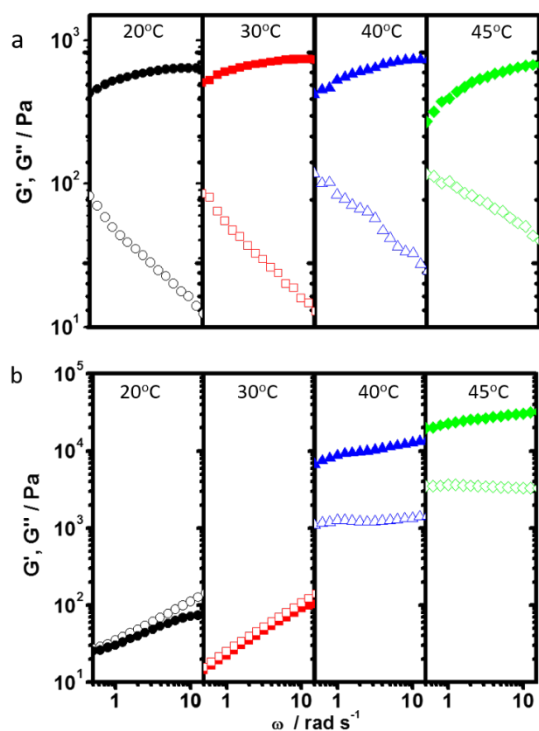


Figure 6 - Frequency dependence (strain amplitude=2%) of storage modulus (G' , solid symbols) and loss modulus (G'' , open symbols) at various temperatures (black circles for 20 °C, red squares for 30 °C, blue triangles for 40 °C, green diamonds for 45 °C) for aqueous gels containing 5 wt% $B_{20}E_{510}$ in the absence (a) and in the presence of 10 wt% Nafion (b).

Frequency sweeps shown in Figure 6a suggest that the 5 wt% aqueous solution of $B_{20}E_{510}$ forms a gel from 20 to 45 °C and the G' show a maximum value of 800 Pa ($\omega=1$ rad/s) at 30 °C. Low G' values in, otherwise immobile, gels close to their critical gel

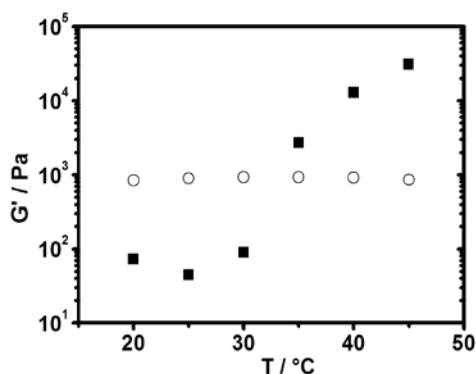


Figure 7 - Temperature dependence of storage modulus G' ($\omega=1$ rad/s, strain amplitude=2%) for aqueous gels containing 5 wt% $B_{20}E_{510}$ in the absence (open circles) and in the presence of 10 wt% Nafion (solid squares). The data were read off from frequency sweeps measurements.

concentration, have been reported previously for copolymers with long E blocks²⁹. As seen in Figure 6b, introduction of 10 wt% Nafion allows the formation of mechanically robust hydrogels with G' higher than 9 kPa and 23 kPa ($\omega=1$ rad/s) at $T=40$ °C and 45 °C. At 40 °C and 45 °C, G' and G'' are only weakly dependent on frequency, indicating solid-like rheological response.

Figure 7 compares the temperature dependence of G' for 5 wt% $B_{20}E_{510}$ (open circles) and 5 wt% $B_{20}E_{510}$ /10 wt% Nafion (full squares) (the data points at $\omega=1$ rad/s were read off from frequency sweeps and were combined in a single curve). It can be seen that within the temperature range 20 to 30 °C, the hybrid gel shows one order of magnitude lower G' compared to its Nafion-free counterpart, an obvious advantage for injectable applications. At temperature above 30 °C the hybrid undergoes an abrupt (albeit thermally reversible) sol-gel transition that results in the formation of a mechanically robust hydrogel. (Due to the pronounced differences in their viscoelastic properties at 37 °C between the two systems shown in Figure 7, we did not conduct drug release studies). Despite this abrupt phase transformation upon heating, SAXS patterns shown in Figure 8 indicate that the structure of the system lacks long range order at 15 °C as expected for a fluid, but this observation remains unaltered at 45 °C, even though the hydrogel behaves rheologically as a solid-like material. With respect to the 5 wt% $B_{20}E_{510}$, we note that the bcc structure of this type of super-swollen gels close to their critical gel concentration has been confirmed so far only by SANS measurements⁴¹, while our SAXS data did not show any refractive peaks.

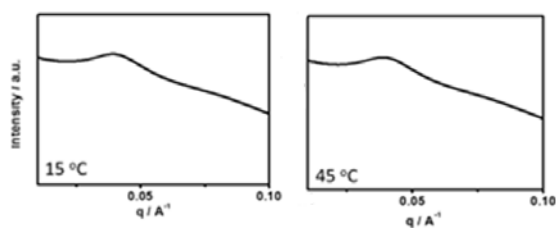


Figure 8 - SAXS patterns of an aqueous gel containing 5 wt% B₂₀E₅₁₀ in the presence of 10 wt% Nafion at the temperatures indicated.

Conclusions

In water, Nafion and PEO based copolymers undergo synergistic mixing as evident by light scattering and QCM-D experiments. At higher concentrations the supramolecular assemblies exhibit an abrupt sol-gel transition below body temperature, generating thermoreversible hydrogels. The 5 wt% B₂₀E₅₁₀/10 wt% Nafion hybrid hydrogel at body temperature exhibits significantly improved mechanical strength compared to its Nafion-free counterpart. Moreover, the hybrid E₁₉P₆₉E₁₉/Nafion gel exhibits dramatically improved drug release profile *in vitro* over a prolonged period of time. Those biocompatible systems offer exciting opportunities for the development of a new generation of super-tough nanogels and bioinks.

Acknowledgements

We thank Diamond Light Source for access to beamline I22 (SM 10168) that contributed to the results presented here. In particular, we wish to thank Dr Nick Terrill and Dr Olga Shebanova for their constant support during our visit to synchrotron facilities. W. K. and J.S. (from Adam Mickiewicz University in Poznan, Poland) were sponsored by the Erasmus mobility program to work in U.K.

References

- [1] A.S. Hoffman, Stimuli-responsive polymers: Biomedical applications and challenges for clinical translation, *Adv. Drug Deliv. Rev.* 65 (2013) 10–16. doi:10.1016/j.addr.2012.11.004.
- [2] T.R. Hoare, D.S. Kohane, Hydrogels in drug delivery: Progress and challenges, *Polymer (Guildf)*. 49 (2008) 1993–2007. doi:10.1016/j.polymer.2008.01.027.
- [3] J. Kopecek, Hydrogel biomaterials: A smart future?, *Biomaterials*. 28 (2007) 5185–92. doi:10.1016/j.biomaterials.2007.07.044.
- [4] M.C. Koetting, J.T. Peters, S.D. Steichen, N.A. Peppas, Stimulus-responsive hydrogels: Theory, modern advances, and applications, *Mater. Sci. Eng. R Reports*. 93 (2015) 1–49. doi:10.1016/j.mser.2015.04.001.
- [5] C. Tsitsilianis, Responsive Reversible Hydrogels from associative “smart” macromolecules, *Soft Matter*. 6 (2010) 2372–88. doi:10.1039/b923947b.
- [6] K.H. Bae, L.-S. Wang, M. Kurisawa, Injectable biodegradable hydrogels: Progress and challenges, *J. Mater. Chem. B*. 1 (2013) 5371–88. doi:10.1039/c3tb20940g.
- [7] L. Yu, J. Ding, Injectable hydrogels as unique biomedical materials., *Chem. Soc. Rev.* 37 (2008) 1473–81. doi:10.1039/b713009k.
- [8] X. Xu, A.K. Jha, D.A. Harrington, M.C. Farach-Carson, X. Jia, Hyaluronic Acid-Based Hydrogels: from a Natural Polysaccharide to Complex Networks, *Soft Matter*. 8 (2012) 3280–94. doi:10.1039/C2SM06463D.
- [9] C. Vinatier, O. Gauthier, A. Fatimi, C. Merceron, M. Masson, A. Moreau, F. Moreau, B. Fella, P. Weiss, J. Guicheux, An injectable cellulose-based hydrogel for the transfer of autologous nasal chondrocytes in articular cartilage defects, *Biotechnol. Bioeng.* 102 (2009) 1259–67. doi:10.1002/bit.22137.
- [10] A.M. Jonker, D.W.P.M. Löwik, J.C.M. Van Hest, Peptide- and protein-based hydrogels, *Chem. Mater.* 24 (2012) 759–73. doi:10.1021/cm202640w.
- [11] H. Tan, C.M. Ramirez, N. Miljkovic, H. Li, J.P. Rubin, K.G. Marra, Thermosensitive injectable hyaluronic

- acid hydrogel for adipose tissue engineering, *Biomaterials*. 30 (2009) 6844–53. doi:10.1016/j.biomaterials.2009.08.058.
- [12] A.P. Constantinou, T.K. Georgiou, Tuning the gelation of thermoresponsive gels, *Eur. Polym. J.* 78 (2016) 366–75. doi:10.1016/j.eurpolymj.2016.02.014.
- [13] P. Alexandridis, J.F. Holzwarth, T.A. Hatton, Micellization of Poly(ethylene oxide)-Poly(propylene oxide)-Poly(ethylene oxide) Triblock Copolymers in Aqueous Solutions: Thermodynamics of Copolymer Association., *Macromolecules*. 27 (1994) 2414–2425. doi:10.1021/ma00087a009.
- [14] C. Booth, D. Attwood, Effects of block architecture and composition on the association properties of poly(oxyalkylene) copolymers in aqueous solution, *Macromol. Rapid Commun.* 21 (2000) 501–27. doi:10.1002/1521-3927(20000601)21:9<501::AID-MARC501>3.0.CO;2-R.
- [15] L. Yu, J. Ding, Injectable hydrogels as unique biomedical materials., *Chem. Soc. Rev.* 37 (2008) 1473–81. doi:10.1039/b713009k.
- [16] N.E. Fedorovich, I. Swennen, J. Girones, L. Moroni, C.A. Van Blitterswijk, E. Schacht, J. Alblas, W.J.A. Dhert, Evaluation of photocrosslinked lutrol hydrogel for tissue printing applications, *Biomacromolecules*. 10 (2009) 1689–96. doi:10.1021/bm801463q.
- [17] H.J. Chung, Y. Lee, T.G. Park, Thermo-sensitive and biodegradable hydrogels based on stereocomplexed Pluronic multi-block copolymers for controlled protein delivery, *J. Control. Release*. 127 (2008) 22–30. doi:10.1016/j.jconrel.2007.12.008.
- [18] Y. Lee, H.J. Chung, S. Yeo, C.-H. Ahn, H. Lee, P.B. Messersmith, T.G. Park, Thermo-sensitive, injectable, and tissue adhesive sol–gel transition hyaluronic acid - pluronic composite hydrogels prepared from bio-inspired catechol-thiol reaction, *Soft Matter*. 6 (2010) 977. doi:10.1039/b919944f.
- [19] K.A. Mauritz, R.B. Moore, State of understanding of Nafion, *Chem. Rev.* 104 (2004) 4535–85. doi:10.1021/cr0207123.
- [20] A. Kelarakis, R.H. Alonso, H. Lian, E. Burgaz, L. Estevez, E.P. Giannelis, Nanohybrid nafion membranes for fuel cells, *ACS Symp. Ser.* 1034 (2010). doi:10.1021/bk-2010-1034.ch012.
- [21] R.F.B. Turner, D.J. Hamisont, R. V Rajotte, Preliminary in vivo biocompatibility studies on perfluorosulphonic acid polymer membranes for biosensor applications, *Biomaterials*. 12 (1991) 361–68. doi:10.1016/0142-9612(91)90003-S.
- [22] R.F.B. Turner, C.S. Sherwood, Biocompatibility of Perfluorosulfonic Acid Polymer Membranes for Biosensor Applications, *Diagnostic Biosens. Polym.* 17 (1994) 211–21. doi:10.1021/bk-1994-0556.ch017.
- [23] P. Hashemi, P.L. Walsh, T.S. Guillot, J. Gras-Najjar, P. Takmakov, F.T. Crews, R.M. Wightman, Chronically implanted, nafion-coated Ag/AgCl reference electrodes for neurochemical applications, *ACS Chem. Neurosci.* 2 (2011) 658–66. doi:10.1021/cn2000684.
- [24] D. Chen, C. Wang, W. Chen, Y. Chen, J.X.J. Zhang, PVDF-Nafion nanomembranes coated microneedles for in vivo transcutaneous implantable glucose sensing, *Biosens. Bioelectron.* 74 (2015) 1047–52. doi:10.1016/j.bios.2015.07.036.
- [25] R.F. Vreeland, C.W. Atcherley, W.S. Russell, J.Y. Xie, D. Lu, N.D. Laude, F. Porreca, M.L. Heien, Biocompatible PEDOT:Nafion composite electrode coatings for selective detection of neurotransmitters in vivo, *Anal. Chem.* 87 (2015) 2600–2607. doi:10.1021/ac502165f.
- [26] Z. Dai, H. Mohwald, Highly Stable and Biocompatible Nafion-Based Capsules with Controlled Permeability for Low-Molecular-Weight Species, *Chem. Eur. J.* 20 (2002) 4751–55. doi:10.1002/1521-3765(20021018)8:20.
- [27] A. Kelarakis, E.P. Giannelis, Nafion as cosurfactant: Solubilization of nafion in water in the

- presence of pluronics, *Langmuir*. 27 (2011) 554–60. doi:10.1021/la103318u.
- [28] A. Kellarakis, M.J. Krysmann, Trivial and Non-Trivial Supramolecular Assemblies Based on Nafion, *Colloids Interface Sci. Commun.* 1 (2014) 31–34. doi:10.1016/j.colcom.2014.06.005.
- [29] A. Kellarakis, V. Havredaki, K. Viras, W. Mingvanish, F. Heatley, C. Booth, S.M. Mai, Aqueous solutions and gels of diblock copolymers of 1,2-butylene oxide and ethylene oxide studied by light scattering and rheology, *J. Phys. Chem. B*. 105 (2001) 7384–93. doi:10.1021/jp003364m.
- [30] G. Sauerbrey, Verwendung von Schwingquarzen zur Wagungdiinner Schichten und zur Mikrowagung, *Zeitschrift Fur Phys.* 155 (1959) 206–22. doi:10.1007/BF01337937.
- [31] M. Rodahl, F. Höök, A. Krozer, P. Brzezinski, B. Kasemo, Quartz crystal microbalance setup for frequency and Q - factor measurements in gaseous and liquid environments Quartz crystal microbalance setup for frequency and Q-factor measurements in gaseous and liquid environments, 66 (1995) 3924–30. doi:10.1063/1.1145396.
- [32] J. Hu, V. Baglio, V. Tricoli, A.S. Arico, V. Antonucci, PEO-PPO-PEO triblock copolymer/Nafion blend as membrane material for intermediate temperature DMFCs, *J. Appl. Electrochem.* 38 (2008) 543–50. doi:10.1007/s10800-007-9471-5.
- [33] A. Kellarakis, J.J. Crassous, M. Ballauff, Z. Yang, C. Booth, Micellar spheres in high frequency oscillatory field, *Langmuir*. 22 (2006) 6814–17. doi:10.1021/la0607860.
- [34] N. Goutev, Z. S. Nickolov, G. Georgiev, H. Matsuura, Hydration of a short chain poly(oxyethylene) (C1E2C1) studied by analysis of the O-H Raman band, *J. Chem. Soc., Faraday Trans.* 93 (1997) 3167–71. doi:10.1039/A702629C
- [35] A. Kellarakis, V. Havredaki, C. Booth, Aqueous gels of diblock oxyethylene-oxypropylene copolymers, *Macromol. Chem. Phys.* 204 (2003) 15–21.
- [36] T.G. O'Lenick, X. Jiang, B. Zhao, Thermosensitive Aqueous Gels with Tunable Sol - Gel Transition Temperatures from Thermo- and pH-Responsive Hydrophilic ABA Triblock Copolymer, *Langmuir*. 26 (2010) 8787–96. doi:10.1021/la9045308.
- [37] A. Kellarakis, V. Castelletto, C. Chaibundit, J. Fundin, V. Havredaki, I.W. Hamley, C. Booth, Rheology and structures of aqueous gels of triblock(oxyethylene/oxybutylene/oxyethylene) copolymers with lengthy oxyethylene blocks, *Langmuir*. 17 (2001) 4232–39. doi:10.1021/la0101806.
- [38] R. Chang, Y. Huang, G. Shan, Y. Bao, X. Yun, T. Dong, P. Pan, Alternating poly(lactic acid)/poly(ethylene-co-butylene) supramolecular multiblock copolymers with tunable shape memory and self-healing properties, *Polym. Chem.* 6 (2015) 5899–910. doi:10.1039/C5PY00742A.
- [39] S.S. Kulthe, N.N. Inamdar, Y.M. Choudhari, S.M. Shirolikar, L.C. Borde, V.K. Mourya, Mixed micelle formation with hydrophobic and hydrophilic Pluronic block copolymers: Implications for controlled and targeted drug delivery, *Colloids Surfaces B Biointerfaces*. 88 (2011) 691–96. doi:10.1016/j.colsurfb.2011.08.002.
- [40] G.M. Zentner, R. Rathi, C. Shih, J.C. Mcrea, M. Morgan, S. Weitman, Biodegradable block copolymers for delivery of proteins and water-insoluble drugs, *J. Control. Release*. 72 (2001) 203–15. doi:10.1016/S0168-3659(01)00276-0.
- [41] V. Castelletto, I.W. Hamley, J.S. Pedersen, Small-Angle Neutron Scattering Study of the Structure of Superswollen Micelles Formed by a Highly Asymmetric Poly(oxybutylene)-Poly(oxyethylene) Diblock Copolymer in Aqueous Solution, *Langmuir*. 20 (2004) 2992–94. doi:10.1021/la036